Soft Matter

PAPER

View Article Online
View Journal | View Issue



Cite this: *Soft Matter*, 2015, **11**, 1335

# The influence of amino acid sequence on structure and morphology of polydiacetylene containing peptide fibres†

Maaike Nieuwland, Nicole van Gijzel, Jan C. M. van Hest and Dennis W. P. M. Löwik*

Received 10th October 2014
Accepted 22nd December 2014

DOI: 10.1039/c4sm02241f

www.rsc.org/softmatter

A systematic study was performed on the influence of charge and steric hindrance on the assembly into fibres of a series of pentameric peptides based on the well-known β-sheet forming sequence Gly-Ala-Gly-Ala-Gly, which were N-terminally acylated with pentacosadiynoic acid. To investigate the effect of steric hindrance and charge repulsion on the fibre structure, either the N-terminal or the C-terminal amino acid in the sequence was replaced by a glutamic acid or lysine residue. Furthermore, peptide amphiphiles (PAs) with an amide or a free acid group at the C-terminus were compared. Steric hindrance and charge repulsion were addressed individually by varying the pH during and after fibre preparation. The self-assembled structures were examined with circular dichroism (CD) spectroscopy and transmission electron microscopy (TEM). UV spectroscopy was used to probe the diacetylene packing in the hydrophobic tail, both by polymerisation behaviour and chromatic properties of the polymers. In brief, the assembly was hindered more if the modification was close to the alkyl tail, and glutamic acid brought about a larger effect than lysine. PAs with two charges yielded assemblies which after polymerisation were found to be the most susceptible towards changes in pH, behaving as a colour-based pH sensor. Typically, TEM and UV showed the same trends, indicating that a distorted morphology as observed with TEM is indicative of a poorer molecular packing of the peptide amphiphile fibres, probed *via* the changes in absorption of the polydiacetylene backbone.

## 1. Introduction

Self-assembled protein fibres are abundant in nature. They often play an important role in biological systems, for example as actin filaments in cells but in some cases they can also be related to diseases such as Alzheimers'. In order to mimic the first and prevent the latter, many different types of self-assembled fibres have been extensively investigated. The protein building blocks that form the natural fibres are quite complex biomolecules, and therefore smaller building blocks are often employed. Especially peptide amphiphiles (PAs) that mimic proteins in their assembly behaviour have gained increasing interest over the years.[1–5] Their relative ease of synthesis provides a means of mimicking structure and function of proteins without the challenging production that traditionally accompanies these large biomolecules. Furthermore, insight into important structural and functional features of proteins can be obtained using these small molecules, and their design can easily be varied in order to explore their structure–function relationship. The interesting structural properties combined with the relatively facile functionalization make PA fibres attractive structures to study. A surprisingly large variety of PAs assemble into a fibre-like shape,[6–13] and most are designed by using hydrophobicity as the main driving force, whereas the hydrophilic head group of the amphiphile contains structural or functional information.[14]

These aspects have been well investigated for peptide amphiphiles consisting of an alkyl tail coupled to a peptide moiety. Small changes such as in the length of the hydrophobic tail[15,16] or the presence or absence of a methyl group in the hydrophilic headgroup[17] can have a marked effect on the fibre morphology. The width,[18] helical pitch,[19] preferred superstructure[20] and other parameters can be tuned by small structural changes in the building block.[21]

A particular interesting class of peptide amphiphiles are obtained when diacetylene units are introduced in the alkyl chains. Diacetylenes can be polymerised to highly conjugated polymers with unique chromatic properties and were first described in the early 70s.[22] One of the interesting properties of the resulting highly conjugated polymers is their chromism[23] – their colour can change from mostly blue to red under the influence of external stimuli.[16,24–40] Interestingly, the topochemical polymerisation diacetylenes can only take place if these moieties are closely packed, as may be the case in for

*Radboud University Nijmegen, Institute for Molecules and Materials, Bio-organic Chemistry, Heyendaalseweg 135, 6525 AJ Nijmegen, The Netherlands. E-mail: d.lowik@science.ru.nl; Tel: +31 (0)24 3652382*

† Electronic supplementary information (ESI) available. See DOI: 10.1039/c4sm02241f

example crystals, but also in self-assembled systems.[16,41–45] Systematic studies on assemblies of diacetylene containing amphiphiles elucidated the effect of several molecular parameters on the polymerisability of diacetylenes and the resulting polydiacetylene (PDA) absorption. For PDA peptide amphiphiles the relation between the peptide and structural and chromatic properties of the resulting polymer have however hardly been studied. Therefore, because both the hydrophobic tail and the hydrophilic head group play an important role in packing of the molecules and thus in the properties of the fibre,[16,25,32,34,37,46–58] we anticipated that from the chromatic properties of the PDA polymers structural information, such as the packing of the PAs, could be derived.[16,59]

To investigate the influence of peptide sequence on fibre morphology and polymerisation properties, we started from a well-known β-sheet forming sequence Gly-Ala-Gly-Ala-Gly (GAGAG) found in *Bombyx mori* silk fibroin, employed by our group and others as part of PAs before.[60–64] Because of the small size of the peptide, containing residues without functionality or special characteristics, we expected charge and steric hindrance could be systematically introduced and their consequences studied.

## 2. Experimental section

All starting materials were obtained from commercial suppliers and used as received. Thin layer chromatography (TLC) was performed on Kieselgel F-254 pre-coated silica plates or RP-8 F-254s. Visualization was accomplished with UV light and/or TDM.[65] Column chromatography was carried out on Merck silica gel 60 (230–400 mesh ASTM). $^1$H-NMR spectra were recorded on a Varian Mercury, 400 MHz. DMSO-d5 ($\delta = 2.5$) was used as a shift reference. Mass spectra were recorded on a JEOL AccuTOF-CS spectrometer.

### Synthesis of the amphiphiles

All peptides were prepared by 'standard' solid-phase Fmoc protocols[66] described in brief below.

For the peptides GGo, GEo, EGo and KGo a Wang resin (Bachem D-1250) was used, for GKo a Barlos resin, GGn, GEn and EGn were synthesized on a Breipohl (Bachem D-1600) resin and GKn and KGn on a Sieber resin (Bachem D2040). The exact sequences of these peptides can be found in Fig. 1. The three-letter abbreviations used throughout the text for each compound provides information on the N- and C-terminal amino acid in each sequence (first and second capital letter subsequently) and designates the nature of the C-terminus (o for carboxylic acid or n for amide).

**Coupling of the first amino-acid to a Wang resin.**[67] To couple the first amino acid, the resin was washed three times with dichloromethane and subsequently suspended in dimethylformamide (DMF). Two equivalents of the Fmoc protected amino acid, 4 eq. 1-hydroxybenzotriazole hydrate (HOBt), 2 eq. diisopropylcarbodiimide (DIPCDI) and 2 eq. 4-dimethylaminopyridine were added. The suspension was agitated overnight. After washing of the resin with DMF unreacted groups on the resin were capped with benzoyl chloride and pyridine (1 : 1, 10 eq.). The suspension was subsequently filtered, washed and dried under vacuum. The loading of the first residue was determined by a UV-Vis determination of the Fmoc-content.[68]

**Coupling of the first amino acid to a Sieber.**[69] **or Breipohl resin.** The resin was swollen for 20 min in DMF. The Fmoc group on the resin was removed using 20% piperidine in DMF (3 × 6 min.). After that, the first amino acid was coupled using a normal peptide coupling, as described below ('coupling of subsequent amino acids').

**Coupling of lysine to a Barlos resin.** To the resin in dry dichloromethane, 2.5 eq. DIPEA and 2 eq. Fmoc-Lys(Boc)-OH, dissolved in dry dichloromethane, were added. The solution was agitated 30 min, after which 5 mL MeOH and another 2.5 eq. DIPEA were added to the mixture and the solution was agitated for another 15 min. The loading of the first residue was determined by a UV-Vis determination of the Fmoc-content.[21]

**Coupling of subsequent amino acids and 10,12-pentacosadiynoic acid.** In all subsequent couplings 3 equivalents of the amino acid, 3.3 equivalents DIPCDI and 3.6 equivalents HOBt

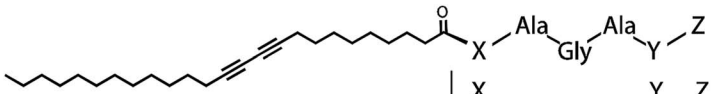


| | | X | Y | Z | Charges depending on pH: acid | neutral | base |
|---|---|---|---|---|---|---|---|
| 1 | GGo | Gly | Gly | OH | 0 | -1 | -1 |
| 2 | GGn | Gly | Gly | $NH_2$ | 0 | 0 | 0 |
| 3 | GEo | Gly | Glu | OH | 0 | -2 | -2 |
| 4 | GEn | Gly | Glu | $NH_2$ | 0 | -1 | -1 |
| 5 | EGo | Glu | Gly | OH | 0 | -2 | -2 |
| 6 | EGn | Glu | Gly | $NH_2$ | 0 | -1 | -1 |
| 7 | GKo | Gly | Lys | OH | +1 | 0 | -1 |
| 8 | GKn | Gly | Lys | $NH_2$ | +1 | +1 | 0 |
| 9 | KGo | Lys | Gly | OH | +1 | 0 | -1 |
| 10 | KGn | Lys | Gly | $NH_2$ | +1 | +1 | 0 |

Fig. 1 Ten PA structures investigated in this study. The PA abbreviations used throughout the manuscript are shown in the left column and are also used for their corresponding fibrous assemblies. In columns on the right the expected charges for each compound in acidic (pH 2), basic (pH 12) and neutral (pH 7) environment are shown. The difference in colour is only to increase the table's legibility.

 

in DMF were used. Deprotections were carried out using 20% piperidine in DMF (3 × 6 min.). After each coupling and deprotection a Kaiser test[70] was performed to check the completeness of the reactions. After removal of the final Fmoc group the peptides were acylated on resin employing 3 equivalents of 10,12-pentacosadiynoic acid dissolved in dichloromethane to which 3.3 equivalents DIPCDI and 3.6 equivalents HOBt in DMF were added.

**Cleavage from a Wang and Breipohl resin.** The peptides GGo, GEo, EGo, KGo, GGn, GEn and EGn were cleaved from the resin by treatment with trifluoroacetic acid/water/triisopropylsilane (95 : 2.5 : 2.5) for two hours, followed by precipitation in ether or by removal of the volatiles *in vacuo*. Column chromatography (eluent: $CHCl_3$/MeOH/$H_2O$ 65 : 25 : 4) and subsequent lyophilisation afforded pure compounds according to $^1$H-NMR, MS and TLC.

**Cleavage from a Sieber resin.** The peptides GKn and KGn were cleaved from the resin using 2% TFA in dichloromethane for 1.5 hours, followed by precipitation in ether or by removal of the volatiles *in vacuo*. Column chromatography (eluent: $CHCl_3$/MeOH/$H_2O$ 65 : 25 : 4) and subsequent lyophilisation afforded pure compounds that were deprotected by treatment with 2 M hydrochloric acid in ethyl acetate for 30 min. Subsequent evaporation, co-evaporation with *tert*-butanol and lyophilisation from acetic acid yielded pure compounds according to $^1$H-NMR, MS and TLC.

**Cleavage from a Barlos resin.** The peptide GKo was cleaved from the resin using a 3 : 1 : 1 mixture of dichloromethane, trifluoroethanol and acetic acid. The protected product was purified using column chromatography (eluent: $CHCl_3$/MeOH/AcOH 65 : 25 : 4) and the remaining Boc protecting group was removed by treatment with 2 M HCl in ethyl acetate for 30 min at room temperature. The solvent was evaporated and co-evaporated with *tert*-butanol. Lyophilisation from acetic acid yielded pure compound according to $^1$H-NMR, MS and TLC.

**Analysis.** The analytical data of the PAs can be found in the ESI† (#1).

### Fibre preparation

The amphiphiles were dispersed in Milli-Q or in glycine buffer (0.1 M, pH 2 or pH 12), at concentrations of either 0.2 or 1.0 mM. The samples were heated to 50 °C for 30 min, followed by 15 min sonication at that temperature. Subsequently, the samples were heated to 90 °C and allowed to cool to room temperature. Polymerisations were carried out on 1 mM samples in an open 15 mL glass vial using a UVASPOT 400T lamp with a sample-light source distance of 22 cm.

### pH variation

The pH of polymerised samples prepared in milliQ was varied using buffers (0.1 M) of pH values between 1 and 13. Glycine buffers (with a concentration of 0.1 M) were used for pH values between 1.6 and 3.0 and between 8.9 and 11.6. Potassium phthalate buffers were used between pH 4.2 and 5.7, a PBS buffer for pH 7.8, citric acid, borax and phosphate buffers for pH 8. For low and high pH hydrochloric acid or sodium hydroxide was added to a concentration of 0.6 M.

### Transmission electron microscopy (TEM)

TEM samples were prepared by floating a carbon-coated copper grid on a peptide amphiphile solution of 0.2 mg mL$^{-1}$ for 5 min, followed by removal of residual water by blotting with a paper filter. The samples were visualized using a JEOL 1010 transmission electron microscope set at an accelerating voltage of 60 kV.

### Circular dichroism (CD) spectroscopy

CD spectra of unpolymerised samples were recorded on a Jasco J-810 spectropolarimeter equipped with a Jasco PTC-423S/L Peltier type temperature control system. The measurements were carried out at a concentration of 0.2 mM using a 1 mm quartz cell. To measure temperature curves, a heating or cooling rate of 3 °C min$^{-1}$ was used. Because the diacetylene functionalities readily polymerised when illuminated with the short wavelengths used for the CD measurements, only every 10 °C spectra were recorded (265–185 nm, 100 nm min$^{-1}$), and the shutter was closed between measurements.

### Infrared (IR) spectroscopy

Solutions of fibrils in water or disassembled amphiphiles in acetic acid were lyophilized and the dry samples were compressed on an ATR crystal with a pressure of 5 N. The spectra were recorded on a Thermo Mattson IR300 spectrometer, fitted with a Harrick ATR unit, accumulating 64 scans per spectrum.

### UV-Vis spectroscopy

Measurements were carried out at a concentration of 1.0 mM using a 1 mm quartz cell. The spectra were recorded on a Varian cary-50 spectrometer, equipped with a water bath to enable temperature changes.

## 3. Results

The starting point for this investigation was pentacosadiynoyl modified GAGAG, amidated at the C-terminus (GGn, structure **2**, Fig. 1). Either the first or the last amino acid was replaced by an ionisable residue which allowed charge to be switched 'on' or 'off' by changing pH. Consequently, charge and steric effects could be addressed individually. For this purpose, lysine – positively charged up to high pH values (p$K_a$ 10.5)[71] and glutamic acid – anionic for pH values higher than 4 (p$K_a$ 3.0–3.4)[71] – were chosen. To investigate the effect of C-terminal ionisability, the resulting five peptide sequences were not only synthesized with an amidated C-terminus but also as a free acid (p$K_a$ 3.0–3.4),[71] introducing an additional pH dependent charge. This brought us to prepare a total of ten peptide amphiphiles (Fig. 1). The assembly properties, morphology, polymerisation behaviour and polymer properties of assemblies of these ten PAs were investigated. GGn, the reference compound described above, was expected to assemble most easily into a β-sheet

structure since neither charges nor bulky residues were present, which would lead to broad fibres not hindered by any unfavourable forces. Furthermore, because of the absence of any ionisable groups, it should assemble into the same morphology independent of pH. The subsequent introduction of charges and steric hindrance *via* either a lysine or glutamic acid residue was expected to disturb the assembly of the amphiphiles. Introduction of either of these residues closer to the alkyl tail was thought to have a larger effect on molecular packing of the amphiphiles and hence the resulting assemblies, an effect also observed by Hartgerink *et al.* for methylation.[17] Furthermore, we examined whether two charges would have a larger effect than just one. Besides morphology, also polymerisation and polymer properties of the diacetylene containing fibre may be influenced by the variation of the peptide sequence. Amphiphiles with a better packing for diacetylene polymerisation to occur were expected to have absorbance at longer wavelength. Following the reasoning above, GGn based PDA is expected to absorb at the longest wavelength while the introduction of charges or steric hindrance would lower this absorption wavelength; an effect expected to be more pronounced if the disturbance is closer to the alkyl tail. However, the exact parameters yielding the longest wavelength absorbance of the polydiacetylene backbone may be different from the parameters yielding the most 'regular' structures observed with electron microscopy which are likely to be the result of a poorer molecular packing of the peptide amphiphiles. In this study, we employed the chromatic properties of the polymers as an indicator for the molecular packing of the molecules. This allowed us to also investigate to what extent the fibre morphology ('large' length scale organisation) is correlated with polydiacetylene colour (molecular scale organisation) and stability of the assemblies.

## Synthesis

All peptide amphiphiles (Fig. 1) were prepared using 'standard' Fmoc solid phase peptide chemistry methods.[66] To obtain peptide amphiphiles (PAs) with a free acid terminus the synthesis was performed on a Wang resin. After cleavage from the resin, purification of the fully deprotected PAs was attempted using column chromatography. For all five compounds (GGo, GEo, EGo, GKo and KGo), purification was troublesome. Acidification by addition of a few percent acetic acid in the eluent improved column chromatography purification by neutralizing the free acid group. Even for KGo this purification was possible, although the lysine side-chain is positively charged under acidic conditions. Only GKo remained problematic, however its purification difficulties were solved by using a Barlos resin in which the lysine remained Boc protected after a mild cleavage, which allowed easy purification. Quantitative deprotection of the lysine was performed after purification.

Using a similar strategy, GGn, EGn and GEn were synthesized on a Breipohl resin, yielding amide-terminated, deprotected species after cleavage. To facilitate purification, GKn and KGn were synthesized on a Sieber resin.[69] Like a Barlos resin, a Sieber resin yields protected peptides after cleavage, but now with an amidated C-terminus instead of a free carboxyl terminus. The protected species were purified and deprotected to complete the series of ten PAs.

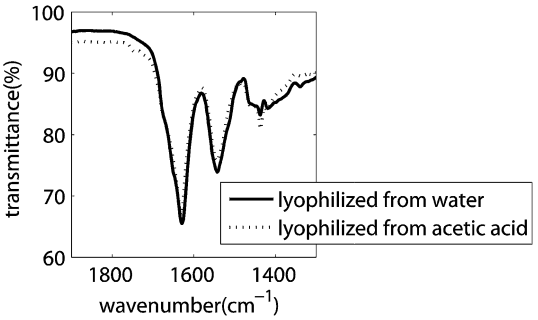


Fig. 2 IR spectrum of GKn lyophilised from water (solid line) and acetic acid (dotted line).

## Conformational analysis of unpolymerised assemblies

First, the peptide conformation in the unpolymerised fibres at neutral pH was investigated using infrared (IR) and circular dichroism (CD) spectroscopy. With CD spectroscopy also the stability of the fibres was examined.

**Infrared (IR) spectroscopy.** Since the sequence of the PAs was inspired on a well-known β-sheet forming peptide, a β-sheet signal was expected for all ten compounds.[60,62] IR measurements corroborated the formation of typical β-sheet structures (sharp peaks at 1540 and 1630 cm$^{-1}$, Fig. 2 and ESI†). The spectra were not conclusive whether the peptides in the β-sheets were in a parallel or antiparallel arrangement. Neither at 1685 cm$^{-1}$ nor at 1645 cm$^{-1}$, wavenumbers indicative for respectively antiparallel and parallel β-sheets, were clear signals observed. However, since an antiparallel arrangement would result in an unfavourable packing of both the hydrophobic tails and the peptides formation of a parallel β-sheet was expected. Moreover, similar PAs studied in our group were also shown to pack in a parallel arrangement.[72] In acetic acid, the PAs were not assembled into fibres (the solution could be filtrated without removing the PAs, which was not possible in water). However, after lyophilisation of the solutions in acetic acid a β-sheet like arrangement was still observed in IR (Fig. 2 and ESI†) indicative of the strong propensity of these molecules to form β-sheet like structures.

**Circular dichroism (CD) spectroscopy.** CD spectroscopy was employed to monitor the conformation of the peptides in the fibres at various temperatures, allowing us to make an estimate of the thermal stability of the assemblies. The expected β-sheet CD signal was obscured by linear dichroism (LD), caused by a random macroscopic alignment in solution resulting in an aberrant CD signal (see ESI†). For all PAs except GGn an ellipticity at room temperature was observed which was clearly distinct from a random coil conformation. The signal indicated assembly presumably in a β-sheet fashion (as observed with IR spectroscopy). GGn was too poorly soluble to obtain a clear CD spectrum.

 

For GEo, EGo, KGn and GKn, the large, LD enhanced signal had disappeared after heating to 90 °C and was replaced by a random coil signal, indicating complete disassembly at this temperature. On the other hand, GGo, KGo, GEn and EGn still showed a signal at 90 °C, though much smaller than at room temperature and more resembling a regular β-sheet signal. The signal decrease was probably caused by partial disassembly, which resulted in smaller, more mobile assemblies, causing the overall directionality and thus the LD effect to diminish. The signal of GKo disappeared upon heating, but did not come back upon cooling which may indicate precipitation or a very slow nucleation process[16] between which we could not discriminate.

The charges and steric hindrance present in assemblies of GEo, EGo, GKn and KGn result in repulsive forces and may explain their lower disassembly temperatures. The same was expected for GEn and especially EGn, with their negative charge and large steric hindrance. For EGn the CD signal at 90 °C was indeed very small and disappeared upon heating to 95 °C. GEn gave a larger signal at 90 °C, but also this PA disassembled when heated to 95 °C. This confirmed the hypothesis that the charge density and steric hindrance were responsible for the disassembly behaviour. The higher stability of GEn compared to EGn can be explained by the absence of much steric hindrance, which allows hydrophobic interactions to maintain fibre integrity. In case of KGo the higher observed stability was also expected, since this PA has a low net charge at neutral pH. A similar result was expected for GKo, but no signal returned upon cooling as mentioned above.

## pH effects on fibre morphology

To compare not only the various PAs at neutral pH but also to investigate the difference in assembly at different pH values, fibres were prepared in a pH 2 glycine buffer, in water and in a pH 12 glycine buffer (see ESI† for representative TEM pictures). The pH of the samples was checked after preparation and samples prepared in water showed a value close to neutral (pH 7).

**Neutral GGn.** Typically, even though no pH sensitive moieties were present in the reference PA GGn, in the pH range studied a large variation in fibre morphology was observed. At low and neutral pH broad, short ribbons were observed (Fig. 3a and b), although in water also a few twisted fibres were detected (arrows in Fig. 3b). In contrast, at high pH much thinner, twisted fibres were present (Fig. 3c), suggesting that the formation of higher ordered aggregates of the assemblies is no longer favourable. The exact cause of this is unknown, but it is probably related to the ions in the solution. Glycine buffers were used for preparation of the fibres at low and high pH. Under basic conditions, glycine may interact with the amphiphiles in the fibres, yielding a shell of glycines around the fibres, introducing steric hindrance and thus causing the formation of thinner, twisted fibres.

**Introduction of charges and steric hindrance.** When the first or last amino acid of GGn was replaced for either a glutamic acid or a lysine, yielding GEn, EGn, GKn and KGn, depending on the pH charge repulsion and/or steric hindrance were introduced in the structure. At neutral pH, both glutamic acid and lysine are charged, and consequently all four structures (GEn, EGn, GKn and KGn) suffered from both steric hindrance and the charge repulsion between side chains of the amphiphiles. Because of these destabilising effects, these four modified PAs assembled into thinner and more twisted fibres compared to GGn. Because the lysine side chain is uncharged at high pH, GGn, GKn and KGn were expected to assemble into broader architectures than GEn and EGn under alkaline conditions. However, no large structural differences between the fibres of these PAs were observed – all assemblies had a thin and twisted morphology in an alkaline environment. This in our opinion reveals the relatively large effect of destabilisation under basic conditions as also observed for the neutral GGn. The charge on GEn and EGn increases upon raising the pH, and consequently fewer fibres were present because of increased solubility and the fibres seemed more twisted. At low pH GEn and EGn formed smaller and more twisted assemblies than GGn. GKn also showed thinner fibres than GGn. Surprisingly, for KGn fibres of the same width as for GGn were observed, although they were longer and seemed more rigid, suggesting charge screening when the charge was positioned close to the alkyl tail. In GKn and KGn only minor changes were observed with pH changes. These results suggest that the incorporation of lysine has a smaller effect than glutamic acid, and that sterics play a larger role than charge repulsion.

**'Interior' *versus* 'exterior' functionalisation.** When EGn was compared with GEn and KGn with GKn, here referred to 'interior' *versus* 'exterior' modification, a larger destabilisation might be expected for modifications closer to the alkyl tail ('interior') as packing of the alkyl chains could become

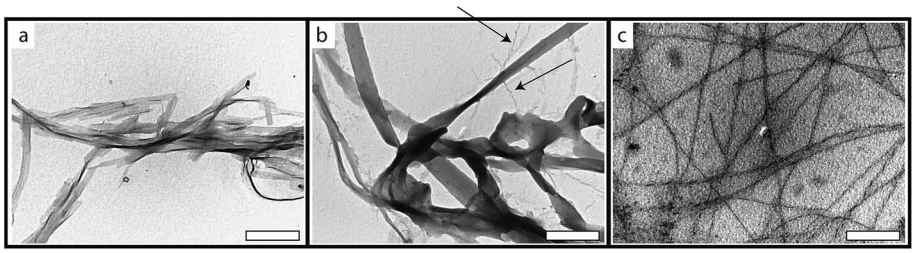


Fig. 3 TEM of GGn. Assemblies prepared (a) at pH 2, (b) in Milli Q (the arrows point to a few of the thin fibres present), (c) at pH 12. The white bars represent 500 nm.

hampered. Indeed, EGn showed a less defined fibre morphology than GEn. This effect was more pronounced when the charge was increased, *i.e.* at higher pH. However, when the morphologies of GKn and KGn were compared at different pH, surprising observations were made. Under acidic conditions, GKn assembled into thinner, longer fibres than KGn. Furthermore, in water and basic solution no large differences between the GKn and KGn assemblies were observed. This result was the opposite effect as found for GEn *versus* EGn, for which was observed that functionalization close to the alkyl tail hampers fibre assembly. A possible explanation could be a more effective charge screening in KGn when compared to GKn, but it also suggests the easier accommodation of lysine compared to glutamic acid in the fibre assembly, since the lysine has a smaller effect when incorporated close to the alkyl tail. Close to the alkyl tail steric hindrance seems to have a larger influence on the morphology than charges, since the charges are more effectively screened, while far from the alkyl tail the (solvent-exposed) charges play a larger role.

**Acid *versus* amide C-terminus.** Introducing a carboxylic acid group instead of an amide at the C-terminus of the peptide introduced a second ionisable group in the amphiphiles. GGo proved to be only moderately soluble under acidic and neutral conditions, which was also observed for GGn. However, the fibres that formed were thinner and longer for GGo than for GGn. Under acidic conditions, neither of these two PAs are charged (Fig. 1) and therefore their assemblies were expected to display the same morphology. Apparently the carboxylic acid group, even at low pH, had a slightly larger charge density than the amide group causing the fibres to be thinner. Under neutral conditions the same effect was observed, in accordance with the charge present in GGo. At high pH both PAs suffered from the destabilisation described above. However, the influence on the morphology was different. GGo showed sheets with a less defined structure instead of the thin twisted fibres of GGn at high pH (Fig. 4, compare Fig. 3c). The same difference was observed for EGo *versus* EGn.

The charges in the glutamic acid functionalised PAs increased the solubility, *i.e.* the driving force for assembly was decreased. GEo dissolved at high pH, not assembling into fibres at all most likely due to large charge repulsion. At low pH, four out of the five acid-terminated PAs precipitated. Only GKo, in which the absence of repulsion by the acid group was compensated by the positive charge of the lysine yielded fibrous structures in solution rather than precipitate. The lysine of KGo was expected to have the same effect. However, this amphiphile precipitated, confirming the buried character of the lysine charge close to the alkyl tail mentioned earlier.

In summary, the pH has a pronounced effect on the formation of PA assemblies and their morphology (see ESI† for TEM pictures of all compounds at acidic, neutral and basic conditions). Charges and steric hindrance have a larger effect when positioned closer to the alkyl tail. Unexpectedly, the side chain of lysine seemed to be easier accommodated within the fibres than that of glutamic acid with resulting smaller changes in morphology. These observation on morphology have been summarized in Table 1.

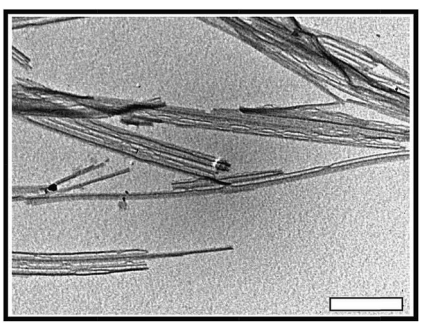

Fig. 4 Fibres of GGo prepared at pH 12. The white bar represents 500 nm.

## Diacetylene polymerisation as indicator for fibre packing and stability

The diacetylene containing alkyl tails were expected to be in an almost crystalline packing, a requirement for the topochemical polymerisation of the diacetylene moieties to occur. The colour of the resulting polydiacetylene was subsequently employed as an indicator for the conformation of the conjugated polymer backbone, which is dependent on the peptide head group conformation and *via* that on the fibre environment.[59]

**Neutral GGn.** Upon illumination of assemblies of GGn the colour of the sample quickly changed from colourless to blue. Because of the poor solubility of the blue suspended particles that formed, UV spectroscopy of this polymer was hampered and we had to restrict ourselves to a visual inspection of any colour changes. Preparation of fibres at low or neutral pH yielded blue polymer after illumination, while at high pH the PA fibres polymerised to a slightly purple colour. Upon heating the solution at neutral pH the polydiacetylene packing changed – the solution turned pink. Upon cooling an almost complete return of the original blue colour was observed, suggesting the reversibility of the structural change of these polydiacetylenes.

**Introduction of charges and steric hindrance.** Replacing the first or last amino acid of the sequence by a lysine or glutamic acid residue yielded fibres which polymerised to materials with different colours at different pH, which suggested a pH dependent diacetylene packing. This is in marked contrast with a similar PA system described earlier by us, in which a GANPNAAG peptide coupled to the same hydrophobic tail resulted in polymerised fibres which yielded the same colour regardless of the conditions.[16,59] Apparently, the peptide plays an important role in the conformational freedom of the diacetylene moieties. Solutions of GEn and EGn prepared at low pH yielded the same result as GGn; a coloured precipitate was observed, which hampered UV-Vis spectrometry. For GEn under neutral and alkaline conditions comparable spectra were observed, while EGn hardly polymerised at pH 12, showing a large difference in structure and solubility between preparations at neutral and high pH for this specific sequence.

**'Interior' *versus* 'exterior' functionalization.** GEn fibres polymerised under neutral conditions absorbed longer

 

Table 1 Summary of the observed morphologies of all PAs at acidic, neutral and basic conditions. The dimensions given are ranges of the width of the PA fibres

| PA | Acidic | Neutral | Basic |
|---|---|---|---|
| (1) GGo | 10–20 nm fibres and 1–5 μm bundles (precipitated) | 10–20 nm and 50–80 nm flat ribbons | 100–500 nm flat ribbons |
| (2) GGn | 100–200 nm fibres and 0.1–1 μm flat ribbons | 10–20 nm fibres and 0.2–2 μm flat ribbons | 50–100 nm twisted fibres |
| (3) GEo | No assembly (precipitated) | 10–20 nm twisted fibres | No assembly |
| (4) GEn | 100–200 nm twisted fibres and 0.5–1 μm bundles | 10–20 nm twisted fibres | Few 100–200 nm twisted fibres |
| (5) EGo | Short 1–3 μm flat ribbons (precipitated) | 10–20 nm twisted fibres aligned in 100–500 nm bundles | 1–2 μm flat ribbons |
| (6) EGn | Few 200–600 nm flat ribbons | 10–20 nm twisted fibres | Few 500 nm ribbons |
| (7) GKo | 100 nm twisted fibres forming up to 3 μm bundles | 10–20 nm twisted fibres forming 50–100 nm bundles | Few 100–300 nm fibres |
| (8) GKn | 100–300 nm twisted fibres | 10–20 nm twisted fibres | 100–300 nm twisted fibres |
| (9) KGo | 1–5 μm flat ribbons (precipitated) | 20–30 nm fibres | 100–300 nm fibres |
| (10) KGn | 0.5–2 μm flat ribbons | 20–30 nm twisted fibres | 50–200 nm twisted fibres |

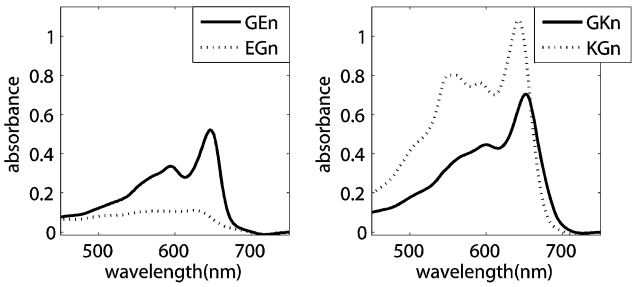


Fig. 5 UV spectra of polymerised GEn, EGn, GKn and KGn, assembled under neutral conditions.

wavelength light than EGn (Fig. 5, left), indicating a better packing of the first diacetylenes. Furthermore, GEn yielded a more intense absorption, indicating the presence of more and possibly longer polymers. The difference between GEn and EGn can be explained from the stronger charge repulsion and increased steric hindrance of the latter because of the position of the glutamic acid in the amphiphile. This is supported by the stronger pH dependence of EGn. In a similar fashion, GKn fibres displayed an absorption at longer wavelength (appeared 'bluer') than KGn. Thus, with the repulsive charges located further away from the colour-determining diacetylene backbone the backbone packed more stably. However, because of solvent-exposed charges in GKn, the amount of assemblies and thus the intensity of the PDA absorption was slightly lower. A glutamic acid residue apparently frustrates the diacetylene packing more than lysine, as shown by a smaller amount (lower absorption intensity) of polymer formed for the glutamic acid containing species.

**Amide *versus* acid C-terminus.** The result of introducing additional charges going from a C-terminal amide to a free acid was apparent, especially at high pH – three of the five compounds with a free acid C-terminus (GEo, EGo and GKo) did not polymerise under basic condition. For GEo and EGo this might be expected because of their double negative charge at high pH, increasing the solubility and impairing assembly. Quite remarkably however, also GKo did not yield a coloured solution after illumination. This peptide was expected to polymerise in a basic environment, since its charge is the same as for GGo, which polymerised under these conditions. Furthermore, the steric hindrance of the lysine was expected not to be problematic, especially since the apparently more sterically hindered KGo did polymerise.

## Polymer properties

Once the fibres were covalently cross-linked upon UV-irradiation they displayed an increased stability compared to the dynamic non-polymerised fibres. Conditions causing disassembly of the fibre before polymerisation will after polymerisation induce stress in the backbone, which has been shown to result in a colour change.[16,59] To explore the colour change of the polymerised fibres upon changing the pH, a solution of hydrochloric acid or sodium hydroxide was added to the fibres. Polymerised samples of GGo, GGn and GKn did not change colour, indicating that once the fibres were polymerised, their structure was not easily disrupted. For GGo and GGn this was in accordance with the polymerisability. Regardless of pH during fibre preparation the colour after polymerisation was similar, showing the pH independence of the alkyl chain conformation in the fibres. On the other hand, GKn showed large differences in absorption spectrum when polymerised at different pH, indicating a diacetylene packing dependent on pH. Therefore, the absence of a colour change after polymerisation was unexpected. Three other compounds (GEn, KGo and KGn) showed a small spectral shift upon pH variation after polymerisation, in accordance with the difference of the colour upon polymerisation at different pH. Polymers made of the last four compounds,

Fig. 6 Colour change from blue to pink when sodium hydroxide was added to a solution of GEo polymers.

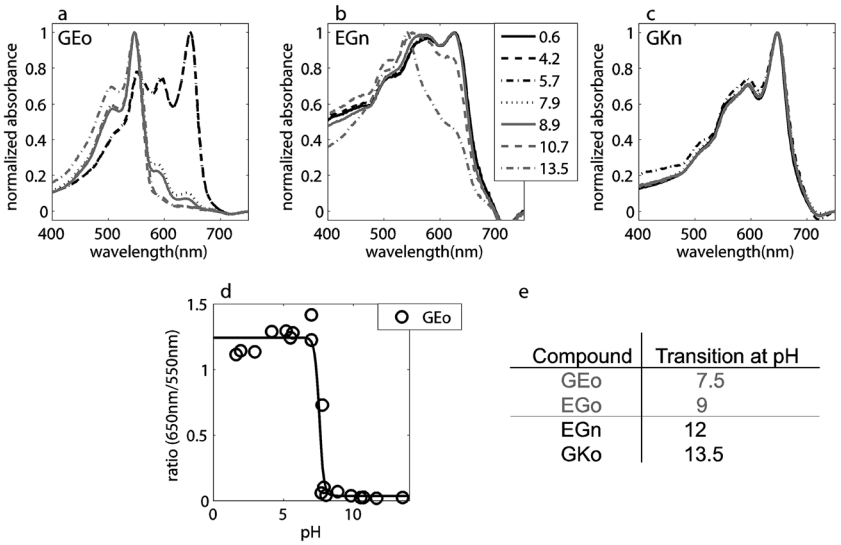


Fig. 7 Variations in absorption upon changing pH. Spectra of (a) GEo, (b) EGn, (c) GKn. Dark lines indicate low, light lines high pH. (d) The ratio of the high-wavelength to the low-wavelength peak for GEo. The line is only to guide the eye. (e) The transition pH of the four compounds with a large colour change.

GEo, EGo, EGn and GKo had a rather large spectral shift with increasing pH. For GEo the diffusion of a sodium hydroxide solution could even be followed by the colour change (Fig. 6). Upon shaking the colour became homogeneously pink. The large colour change was expected, since addition of base before polymerisation prevented these four PAs (GEo, EGo, EGn and GKo) from assembling. The most substantial colour change was observed for GEo, followed by EGo and EGn. The colour change of GKo was the smallest in this series.

The colour change of fibres polymerised in Milli-Q was studied in more detail over a range of pH values between 1 and 14. In Fig. 7 the corresponding UV-Vis spectra are shown for GEo, EGn and GKn which showed respectively a very large, a large and no change in absorption spectrum upon pH variation. In order to quantify the colour change, the ratio between the higher-wavelength and lower-wavelength peak was used. In case of GEo (Fig. 7a) these were the maxima at 650 nm and 550 nm. For each compound the peaks chosen as 'higher' and 'lower' wavelength peaks were at a slightly different position, and therefore the absolute value of the ratio and the sharpness of an eventual colour transition could not be compared between compounds. The peak ratio was plotted against the pH. For the four compounds which showed a large colour change upon addition of a base (GEo, EGo, GKo and EGn), this yielded a colour transition (Fig. 7d for GEo). GEo changed colour at a pH of approximately 7.5, EGo followed at pH 9 and EGn at 12. GKo only changed colour if the pH was raised to 13.5 or higher using NaOH. These pH values followed the same trend as the magnitude of the spectral shift, *i.e.* the compounds which showed the largest colour change (GEo), had their transition point at the lowest pH value. This indicated that either two negative charges in close proximity (GEo) or a charge in a susceptible location, *i.e.* close to the alkyl tail (EGo and EGn) were required for a large colour change. The second charge in EGo did not have a large effect, probably because the charges were too far apart to have a cumulative effect. GKo was least responsive but because of its small amount of charges, the effect was still remarkably large.

## 4. Discussion and conclusions

The effects of steric hindrance and charge repulsion on morphology and molecular packing of peptide amphiphile fibres were investigated. To this end a series of PAs was synthesized based on the pentameric GAGAG, N-terminally functionalised with a diacetylene-containing hydrophobic tail. Either the first or the last glycine in GAGAG was substituted for either lysine or glutamic acid and the C-terminus consisted of a free acid or an amide. In order to separately investigate charge repulsion and steric hindrance, the assemblies were studied at various pH values. The stability (disassembly of the fibres, monitored by CD), showed that the small change of replacing one amino acid or even placing it in a different position within a pentameric peptide has a large influence on the properties. A larger charge resulted in a lower disassembly temperature.

All ten peptide amphiphiles assembled into fibrous structures in aqueous solution. The morphology of the fibres showed striking differences, most likely as a result of the differences in packing. At pH values for which the side chains are charged, both for lysine and glutamic acid charge repulsion between the amphiphiles caused a smaller, more twisted assembly. However, when uncharged, Glu was found to disturb the packing more than Lys – there were large differences between the morphologies of assemblies of GEn and EGn, while the morphological differences between GKn and KGn were negligible.

The diacetylene functionality in the hydrophobic tail of the peptide provided the opportunity to polymerise the assemblies,

 

yielding highly coloured polymers. Their colour and responsiveness to external stimuli was exploited to obtain information about the molecular packing of the amphiphiles within the fibres. Overall the same trend was observed for the diacetylene packing and morphology. Apparently, the distortion of morphology (observed with TEM) correlates with changes in diacetylene packing at a molecular scale (probed by UV spectroscopy). For example in GGn the morphology changed from broad ribbons at low and neutral pH to small, twisted fibres at high pH, while the colour changed from blue when polymerised at low or neutral pH to purple when prepared at high pH. Furthermore, both morphology and colour after polymerisation of GEn and EGn indicated a worse packing for EGn, which yielded a less intense absorption, a lower wavelength maximum absorption and a more distorted morphology. However, there is an important difference between morphology observed with TEM and the diacetylene packing as observed with UV-Vis spectroscopy. The morphology is mainly determined by the outside of the fibre, while the diacetylene packing is sensitive to the changes closer to the hydrophobic tail. With TEM, broader assemblies were observed for KGn than for GKn, suggesting a better packing of the former. On the other hand, GKn had a higher wavelength absorbance than KGn, which suggested a better packing of the diacetylenes for GKn. This typical difference between effect of peripheral and internal functionalization was only visible in the difference between KGn and GKn. The other amphiphiles showed the same trend both in morphology and colour.

When the pH of the solutions was changed after polymerisation, only peptides with multiple charges or a charge close to the alkyl tail induced a structural change in the head group large enough to also cause stress in the backbone of the polydiacetylene. The magnitude of the colour change followed the number of charges. A large change, with a colour transition at low pH, was observed for GEo, in which the charge effect is cumulative, followed by EGo and EGn. Also GKo showed a colour transition, although only at high pH. The relatively high pH responsiveness of this PA was unexpected, but was also observed in morphological analysis (TEM) and stability (CD spectroscopy).

To conclude, the peptide amphiphile assembly is controlled by a subtle interplay between hydrophobic forces, hydrogen bonds, charge interactions and steric hindrance. Notwithstanding the complexity of the fibre formation, a few rather simple rules are formulated which are generally complied. Firstly, without steric hindrance or charge repulsion, these PAs assemble into broad fibres, with an almost perfect diacetylene packing. Secondly, a disturbance close to the alkyl tail has a larger effect than one further away from the alkyl tail. Thirdly, glutamic acid causes a larger disturbance than lysine, and lastly, to have a cooperative effect of charges, they need to be close to each other. These rules of thumb might be used to design new PA based materials of which the sensitivity towards their environment can be tuned.[73] We intend to employ this type of PA fibres as biocompatible sensors.[35,74]

## References

1 X. Zhao, F. Pan, H. Xu, M. Yaseen, H. Shan, C. A. E. Hauser, S. Zhang and J. R. Lu, *Chem. Soc. Rev.*, 2010, **39**, 3480–3498.
2 H. Cui, M. J. Webber and S. I. Stupp, *Pept. Sci.*, 2010, **94**, 1–18.
3 F. Versluis, H. R. Marsden and A. Kros, *Chem. Soc. Rev.*, 2010, **39**, 3434–3444.
4 I. W. Hamley, *Soft Matter*, 2011, **7**, 4122–4138.
5 D. W. P. M. Löwik and J. C. M. van Hest, *Chem. Soc. Rev.*, 2004, **33**, 234–245.
6 S. Matsumura, S. Uemura and H. Mihara, *Chem.–Eur. J.*, 2004, **10**, 2789–2794.
7 M. G. Ryadnov and D. N. Woolfson, *Angew. Chem., Int. Ed.*, 2003, **42**, 3021–3023.
8 M. R. Ghadiri, J. R. Granja, R. A. Milligan, D. E. McRee and N. Khazanovich, *Nature*, 1993, **366**, 324–327.
9 C. Wang, L. X. Huang, L. J. Wang, Y. K. Hong and Y. L. Sha, *Biopolymers*, 2007, **86**, 23–31.
10 Y. Kikkawa, E. Koyama, S. Tsuzuki, K. Fujiwara, K. Miyake, H. Tokuhisa and M. Kanesato, *Chem. Commun.*, 2007, 1343–1345.
11 J. D. Hartgerink, E. Beniash and S. I. Stupp, *Science*, 2001, **294**, 1684–1688.
12 A. Brizard, R. K. Ahmad and R. Oda, *Chem. Commun.*, 2007, 2275–2277.
13 S. R. Diegelmann, J. M. Gorham and J. D. Tovar, *J. Am. Chem. Soc.*, 2008, **130**, 13840–13841.
14 A. Aggeli, M. Bell, L. M. Carrick, C. W. G. Fishwick, R. Harding, P. J. Mawer, S. E. Radford, A. E. Strong and N. Boden, *J. Am. Chem. Soc.*, 2003, **125**, 9619–9628.
15 D. W. P. M. Löwik, J. Garcia-Hartjes, J. T. Meijer and J. C. M. van Hest, *Langmuir*, 2005, **21**, 524–526.
16 M. van den Heuvel, D. W. P. M. Löwik and J. C. M. van Hest, *Biomacromolecules*, 2008, **9**, 2727–2734.
17 S. E. Paramonov, H. W. Jun and J. D. Hartgerink, *J. Am. Chem. Soc.*, 2006, **128**, 7291–7298.
18 H. Xu, J. Wang, S. Y. Han, J. Q. Wang, D. Y. Yu, H. Y. Zhang, D. H. Xia, X. B. Zhao, T. A. Waigh and J. R. Lu, *Langmuir*, 2009, **25**, 4115–4123.
19 L. C. Palmer and S. I. Stupp, *Acc. Chem. Res.*, 2008, **41**, 1674–1684.
20 K. Channon and C. E. MacPhee, *Soft Matter*, 2008, **4**, 647–652.
21 H. Cui, A. G. Cheetham, E. T. Pashuck and S. I. Stupp, *J. Am. Chem. Soc.*, 2014, **136**, 12461–12468.
22 G. Wegner, *Makromol. Chem.*, 1972, **154**, 35–48.
23 X. Sun, T. Chen, S. Huang, L. Li and H. Peng, *Chem. Soc. Rev.*, 2010, **39**, 4244–4257.
24 B. Tieke, G. Lieser and G. Wegner, *J. Polym. Sci., Part A: Polym. Chem.*, 1979, **17**, 1631–1644.
25 Q. Cheng, M. Yamamoto and R. C. Stevens, *Langmuir*, 2000, **16**, 5333–5342.
26 Z. Z. Yuan, C. W. Lee and S. H. Lee, *Angew. Chem., Int. Ed.*, 2004, **43**, 4197–4200.
27 A. Potisatityuenyong, R. Rojanathanes, G. Turncharern and M. Sukwattanasinitt, *Langmuir*, 2008, **24**, 4461–4463.

28 S. Wu, L. F. Niu, J. Shen, Q. J. Zhang and C. Bubeck, *Macromolecules*, 2009, **42**, 362–367.
29 N. Mino, H. Tamura and K. Ogawa, *Langmuir*, 1992, **8**, 594–598.
30 W. D. Zhou, Y. L. Li and D. B. Zhu, *Chem.–Asian J.*, 2007, **2**, 222–229.
31 U. Jonas, K. Shah, S. Norvez and D. H. Charych, *J. Am. Chem. Soc.*, 1999, **121**, 4580–4588.
32 J. Song, J. S. Cisar and C. R. Bertozzi, *J. Am. Chem. Soc.*, 2004, **126**, 8459–8465.
33 J. Song, Q. Cheng, S. Kopta and R. C. Stevens, *J. Am. Chem. Soc.*, 2001, **123**, 3205–3213.
34 S. Okada, S. Peng, W. Spevak and D. Charych, *Acc. Chem. Res.*, 1998, **31**, 229–239.
35 D. H. Charych, J. O. Nagy, W. Spevak and M. D. Bednarski, *Science*, 1993, **261**, 585–588.
36 A. Lio, A. Reichert, D. J. Ahn, J. O. Nagy, M. Salmeron and D. H. Charych, *Langmuir*, 1997, **13**, 6524–6532.
37 Y. K. Jung, T. W. Kim, J. Kim, J. M. Kim and H. G. Park, *Adv. Funct. Mater.*, 2008, **18**, 701–708.
38 J. Lee, H. J. Kim and J. Kim, *J. Am. Chem. Soc.*, 2008, **130**, 5010–5011.
39 S. W. Lee, C. D. Kang, D. H. Yang, J. S. Lee, J. M. Kim, D. J. Ahn and S. J. Sim, *Adv. Funct. Mater.*, 2007, **17**, 2038–2044.
40 B. A. Pindzola, A. T. Nguyen and M. A. Reppy, *Chem. Commun.*, 2006, 906–908.
41 E. Jahnke, A. S. Millerioux, N. Severin, J. P. Rabe and H. Frauenrath, *Macromol. Biosci.*, 2007, **7**, 136–143.
42 E. Jahnke, I. Lieberwirth, N. Severin, J. P. Rabe and H. Frauenrath, *Angew. Chem., Int. Ed.*, 2006, **45**, 5383–5386.
43 D. W. P. M. Löwik, I. O. Shklyarevskiy, L. Ruizendaal, P. C. M. Christianen, J. C. Maan and J. C. M. van Hest, *Adv. Mater.*, 2007, **19**, 1191–1195.
44 L. Hsu, G. L. Cvetanovich and S. I. Stupp, *J. Am. Chem. Soc.*, 2008, **130**, 3892–3899.
45 S. R. Diegelmann and J. D. Tovar, *Macromol. Rapid Commun.*, 2013, **34**, 1343–1350.
46 B. Hupfer and H. Ringsdorf, *Chem. Phys. Lipids*, 1983, **33**, 263–282.
47 H. Tachibana, Y. Yamanaka, H. Sakai, M. Abe and M. Matsumoto, *Macromolecules*, 1999, **32**, 8306–8309.
48 Q. Huo, K. C. Russell and R. M. Leblanc, *Langmuir*, 1999, **15**, 3972–3980.
49 P. Deb, Z. Z. Yuan, L. Ramsey and T. W. Hanks, *Macromolecules*, 2007, **40**, 3533–3537.
50 B. Tieke, H. J. Graf, G. Wegner, B. Naegele, H. Ringsdorf, A. Banerjie, D. Day and J. B. Lando, *Colloid Polym. Sci.*, 1977, **255**, 521–531.
51 J. Yoon, Y. S. Jung and J. M. Kim, *Adv. Funct. Mater.*, 2009, **19**, 209–214.
52 M. Masuda, T. Hanada, Y. Okada, K. Yase and T. Shimizu, *Macromolecules*, 2000, **33**, 9233–9238.
53 J. H. Fuhrhop, P. Schnieder, E. Boekema and W. Helfrich, *J. Am. Chem. Soc.*, 1988, **110**, 2861–2867.
54 Q. Cheng and R. C. Stevens, *Langmuir*, 1998, **14**, 1974–1976.
55 N. R. Lee, C. J. Bowerman and B. L. Nilsson, *Biomacromolecules*, 2013, **14**, 3267–3277.
56 K. Tomizaki, T. Ikawa, S.-A. Ahn, S. Yamazoe and T. Imai, *Chem. Lett.*, 2012, **41**, 549–551.
57 D. Roberts, C. Rochas, A. Saiani and A. F. Miller, *Langmuir*, 2012, **28**, 16196–16206.
58 Q. Huo, S. P. Wang, A. Pisseloup, D. Verma and R. M. Leblanc, *Chem. Commun.*, 1999, 1601–1602.
59 M. van den Heuvel, D. W. P. M. Löwik and J. C. M. van Hest, *Biomacromolecules*, 2010, **11**, 1676–1683.
60 H. Guo, J. Zhang, T. Xu, Z. Zhang, J. Yao and Z. Shao, *Biomacromolecules*, 2013, **14**, 2733–2738.
61 H.-A. Klok, A. Rosler, G. Gotz, E. Mena-Osteritz and P. Bauerle, *Org. Biomol. Chem.*, 2004, **2**, 3541–3544.
62 R. Matmour, I. De Cat, S. J. George, W. Adriaens, P. Leclere, P. H. H. Bomans, N. Sommerdijk, J. C. Gielen, P. C. M. Christianen, J. T. Heldens, J. C. M. van Hest, D. W. P. M. Löwik, S. De Feyter, E. W. Meijer and A. Schenning, *J. Am. Chem. Soc.*, 2008, **130**, 14576–14583.
63 L. Ayres, P. Hans, J. Adams, D. W. P. M. Löwik and J. C. M. van Hest, *J. Polym. Sci., Part A: Polym. Chem.*, 2005, **43**, 6355–6366.
64 J. M. Smeenk, M. B. J. Otten, J. Thies, D. A. Tirrell, H. G. Stunnenberg and J. C. M. van Hest, *Angew. Chem., Int. Ed.*, 2005, **44**, 1968–1971.
65 E. V. Arx, M. Faupel and M. Brugger, *J. Chromatogr.*, 1976, **120**, 224–228. See also ESI† for a procedure in English.
66 G. B. Fields and R. L. Noble, *Int. J. Pept. Protein Res.*, 1990, **35**, 161–214.
67 J. W. Van Nispen, J. P. Polderdijk and H. M. Greven, *Recl. Trav. Chim. Pays-Bas*, 1985, **104**, 99–100.
68 M. Gude, J. Ryf and P. D. White, *Lett. Pept. Sci.*, 2002, **9**, 203–206.
69 P. Sieber, *Tetrahedron Lett.*, 1987, **28**, 6147–6150.
70 E. Kaiser, R. I. Colescot, C. D. Bossinge and P. I. Cook, *Anal. Biochem.*, 1970, **34**, 595–598.
71 N. L. Benoiton, *Chemistry of Peptide Synthesis*, CRC Press, Boca Raton, 2006.
72 M. Nieuwland, L. Ruizendaal, A. Brinkmann, L. Kroon-Batenburg, J. C. M. van Hest and D. W. P. M. Löwik, *Faraday Discuss.*, 2013, **166**, 361.
73 D. J. Ahn, S. Lee and J.-M. Kim, *Adv. Funct. Mater.*, 2009, **19**, 1483–1496.
74 X. Chen, G. Zhou, X. Peng and J. Yoon, *Chem. Soc. Rev.*, 2012, **41**, 4610–4630.

 